Formation Mechanism of Chunky Graphite in Heavy-Section Ductile Cast Irons

H. Itofuji
H. Uchikawa
Ube Steel Co., Ltd., Ube City, JAPAN

ABSTRACT

The formation mechanism of a chunky graphite structure in heavy-section ductile cast irons was studied using SEM, TEM, EPMA with colored mapping photo systems, optical microscopy, etc. In this study, the substructure and element segregation was analyzed.

The whole chunky graphite cell was much bigger than other types of graphite. For example, the average size was approximately 0.8 mm3. Furthermore, the chunky graphite cell was complicatedly interconnected, frequently branched, and composed of graphite chips. Each chip had a face of basal plane and a section of prism face of the hexagonal graphite crystal. Therefore, the basal plane was mostly observed on the surface of chunky graphite. Some inclusions were observed in the chunky graphite cell, but it appeared that there was no direct bonding between graphite and inclusion. It was considered that chunky graphite basically possessed the same substructure as CV and spheroidal graphite and would take a similar growth manner. It was observed that all of the graphite nodules in spheroidal graphite structure had a Mg-segregated ring around them in austenite shell. In case of chunky graphite structure, graphite nodules also had the same kind of ring, although the segregation was rather weak, but the high Mg segregation was observed at an area between austenite dendrites and between austenite shell and dendrite. It was considered that chunky graphite would be precipitated if the area of the thermal center in the heavy section lacked available Mg as a gas bubble. This would be a main reason chunky graphite was precipitated. A new theory named "Site Theory" will be proposed in this paper. It was found that all of the graphite formation mechanism in cast iron might be explained by this theory, whether the graphite precipitation occurred in the liquid phase or the solid phase.

INTRODUCTION

In former reports,[1,2] the CV graphite formation mechanism was discussed and a new theory was proposed, although it had not been named at that time yet.

The theory was based on the nature of the properties of graphite precipitation as follows:

1) Graphite dominantly grows along the a-axis of graphite hexagonal crystal, because the energy of carbon bonding in the basal plane is much bigger than that between the basal plane.
2) Graphite has no bonding system with the other elements of cast iron. Actually, graphite floats in the matrix.
3) Graphite can easily and dominantly precipitate at a free surface in cast iron.

The formation mechanism of the other graphites such as spheroidal, flake, and kish graphite could also be explained with this theory. According to some papers,[3–5] it appeared that the chunky graphite formation mechanism would be similar to CV and spheroidal graphite. Therefore, it was considered that the formation mechanism of all the above graphite would be explained by a common theory.

Yingyi[3] and Zhou[4] have reported that spheroidal graphite precipitated at the early stage of the chunky graphite solidification process, that chunky graphite started to form at austenite-residual melt interface at the middle stage of it and continue to the end of the solidification. Zhou[4] additionally mentioned the existence of the melt channel between the chunky graphite end and the residual melt.

Liu[6] has reported that chunky graphite was interconnected and frequently branched and that the substructure observed using SEM was almost similar to spheroidal graphite.

First, chunky graphite was believed as broken pieces of spheroidal graphite.[7–9] But recently, the graphite morphology has come to be able to be observed in detail more and more using advanced SEM, TEM, EPMA, etc. Therefore, many researchers[3,5] have reported that chunky graphite was not pieces of broken spheroidal graphite, but appeared to take a similar formation manner to spheroidal graphite; the manner of spiral[5] or screw[3] dislocation growth.

In this paper, the substructure of chunky graphite and the element segregation of the structure will be discussed and the chunky graphite formation mechanism will be considered under the new theory.

EXPERIMENTAL PROCEDURE

The tendency of the solidification process of cast iron with chunky graphite has already been reported by many researchers[3,4] and, also, the practical precipitation phenomena in foundry is already known by many researchers.[6–12] Therefore, to clear the chunky graphite formation mechanism, the substructure and element segregation were observed as further study.

Substructure Observation

To observe the substructure of chunky graphite in heavy-section ductile cast iron, the chunky graphite cell was extracted from the matrix keeping the small specimen at about 80C in 40% 6N·HClO4 + 60% 8N·HNO_3(aq). Forty percent HF was sometimes added to keep good extraction. After extraction, the chunky graphite cell was repeatedly rinsed with 40% HF, 1.2 N·HCl(aq) and 3% NaOH(aq) before the final rinse with ethyl alcohol.

And then, the chunky graphite cell substructure was observed using SEM and STEM. As the next step, the chunky, graphite cell in ethyl alcohol was vibrated with an ultrasonic washing machine and broken into small pieces. These pieces were also observed in the same way as above.

The microstructure of the specimen used for this experiment is shown in Figure 1. The specimen was taken out from a center of wall thickness with 230 mm in 36-ton ductile cast iron. The chemical composition is shown in Table 1.

Table 1.
Chemical Composition of Extraction and Mapping Analysis Specimen

Structure of specimen	Chemical composition (Wt%)									
	C	Si	Mn	P	S	Ca	Ce	Mg	CE	OI
Chunky graphite (Extraction)	3.40	2.15	0.37	0.043	0.007	0.0026	0.017	0.044	4.12	0.18
Chunky graphite (Mapping analysis)	3.55	2.81	0.35	0.014	0.009	0.0050	0.013	0.049	4.34	0.09
Spheroidal graphite (Mapping analysis)	3.53	2.31	0.27	0.037	0.010	0.0027	0.016	0.051	4.30	0.09

CE = C+1/3Si
OI = Other impurities
= Cr+Ti+Sn+Al+As+Pb+Sb+Bi+Zn+V+Nb

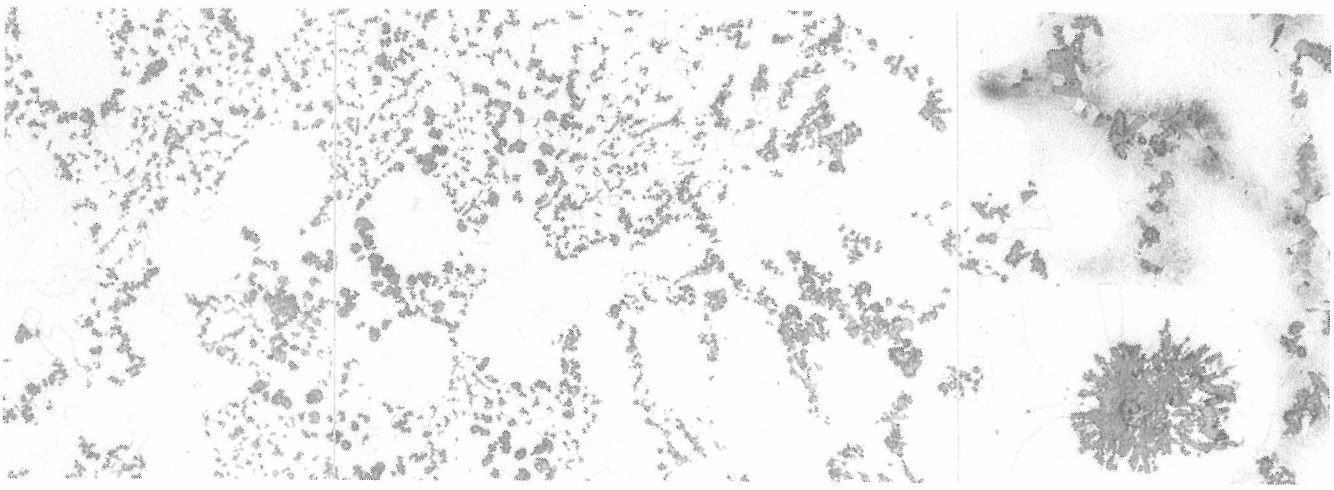

Fig. 1. Microstructure of chunky graphite extracted specimen. Thermal center of wall thickness with 230 mm in 36-ton casting. Etched, 2% Nital (100X).

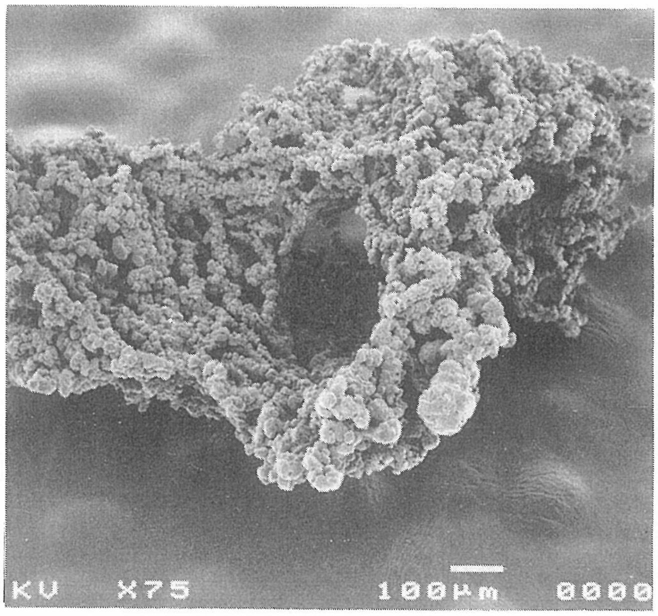

(2a) 75X, SEM

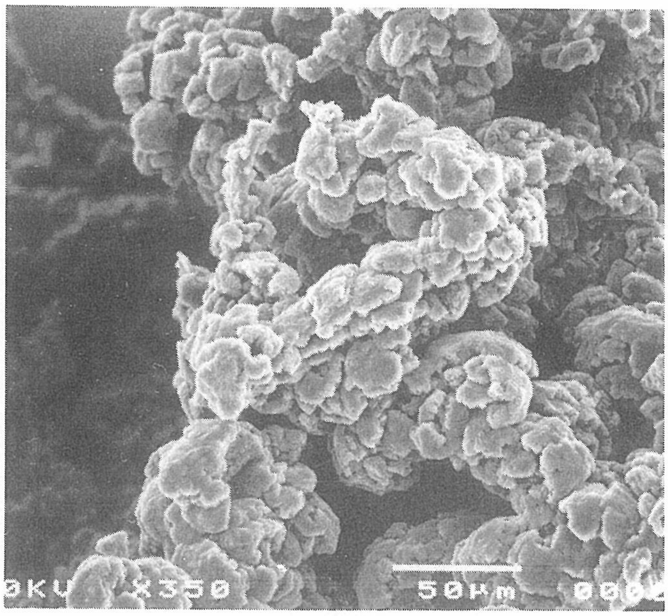

(2b) 350X, SEM

Fig. 2. Chunky graphite cell extracted from matrix.

Analysis of Element Segregation

The segregation of C, Si, Mn, P, S, Ti, Ca, Ce, Mg, O, and N was observed on the chunky graphite structure using EPMA with the color mapping photo system. The area segregated by some elements was also observed with optical microscopy, SEM, and EDAX.

The specimen observed with EPMA was taken out from a thermal center with wall thickness with 210 mm in 4.5-ton ductile cast iron.

The same analysis was done on spheroidal graphite structure as a comparison. The specimen was taken out from 900x900x150^{t} mm test casting. The chemical composition is shown in Table 1.

RESULTS

Substructure of Chunky Graphite

A whole piece of the chunky graphite was much bigger than that of CV and spheroidal graphite and the average size was an outline of approximately 0.8 mm^3, as shown in Figure 2. As mentioned by many researchers,[6] it was clearly observed that chunky graphite was complicatedly interconnected and frequently branched in the cell. Some round space, which may be formed by the existence of austenite dendrite, was observed in the cell. This means that austenite dendrite may relate to the formation mechanism of chunky graphite. More information was observed through high magnification (Fig. 3), and showed that the substructure was quite similar to CV and

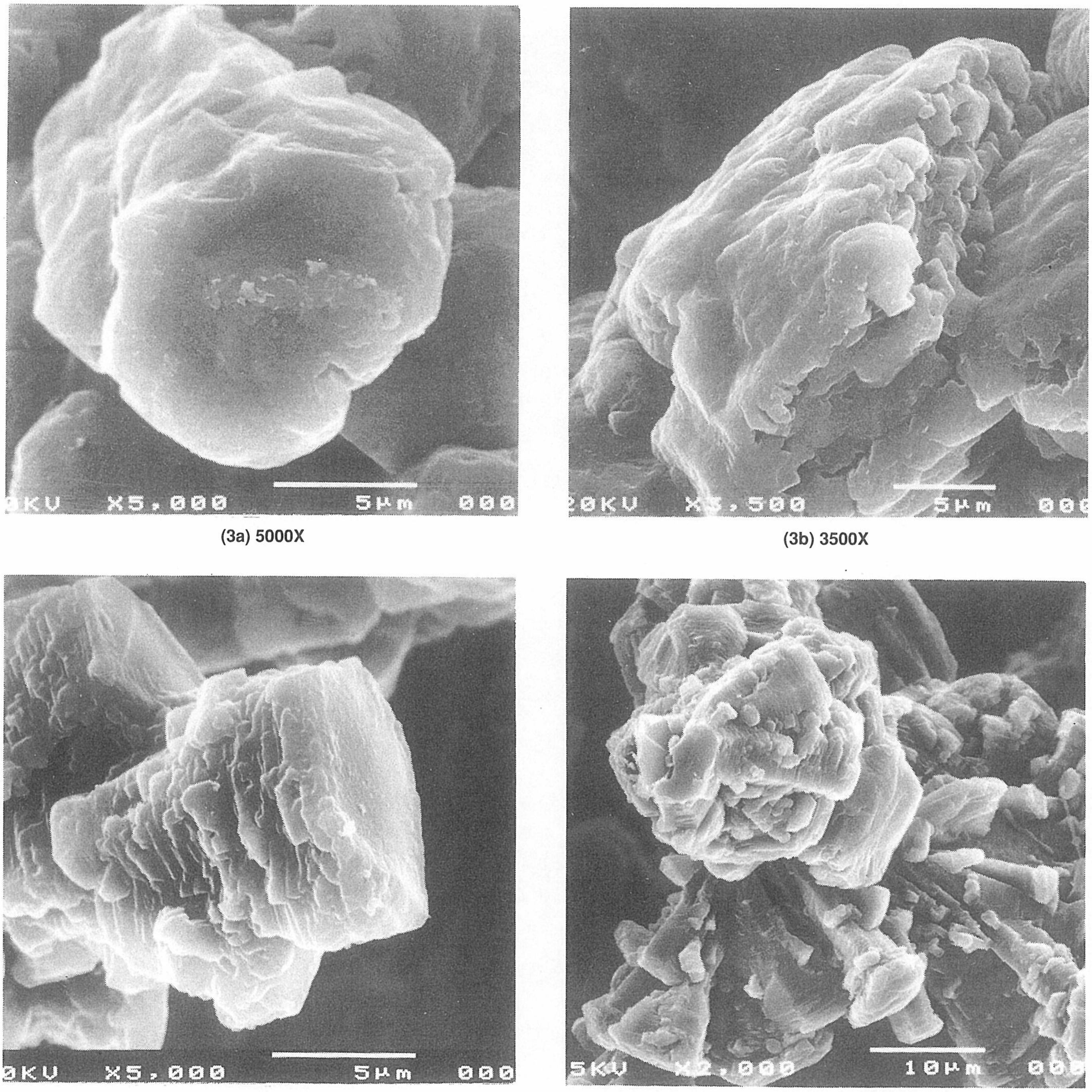

(3a) 5000X

(3b) 3500X

(3c) 5000X

(3d) 2000X

Fig. 3. High magnification of chunky graphite cell extracted from matrix.

spheroidal graphite in appearance. For example, it seemed that chunky graphite was composed of graphite chips, the same as CV and spheroidal graphite.[1]

Actually, the chunky graphite cell was easily broken into small pieces with the ultrasonic vibration. There were two types of pieces, one was a thin chip and another was a thick block layered with many thin chips. These typical chips had a face of basal plane and a section of prism face of the hexagonal graphite crystal, as shown in Figures 4 and 5. It was observed that the surface of chunky graphite was mainly covered with basal plane (Fig. 6), but prism face was exposed at some surfaces, as shown in Figure 3d.

This was quite understandable since the chunky graphite cell was composed of the above graphite chips at random. A lower side of graphite block in Figure 5 was observed with high magnification (100KX) by TEM (Fig. 7) and it was found that the thick block was composed of many thin graphite chips and that each chip's thickness was approximately 2.5 nm. This was equivalent to approximately eight layers of basal plane. Although some chips looked more than 2.5 nm, it was observed that they were just a piling up of the unit chips. Actually, the thicker one was an integral number times of unit thickness.

Spiral-like growth was observed on some ends of chunky graphite, as shown in Figures 3a and 3d. However, they were not actually the spiral growth. It seemed that the spiral growth would be only dislocation in the graphite chip and it would not be a whole process of chunky graphite growth, but only small parts even if it existed.

Thus, it was proved that chunky graphite cell was the result of piling up of thin graphite chips, that the spiral growth did not exist as the behavior of the whole growth process, and that the substructure among CV, spheroidal, and chunky graphite was basically the same. Therefore, it is clear that there would be a common formation mechanism among CV, spheroidal, and chunky graphite.

TEM, 12KX

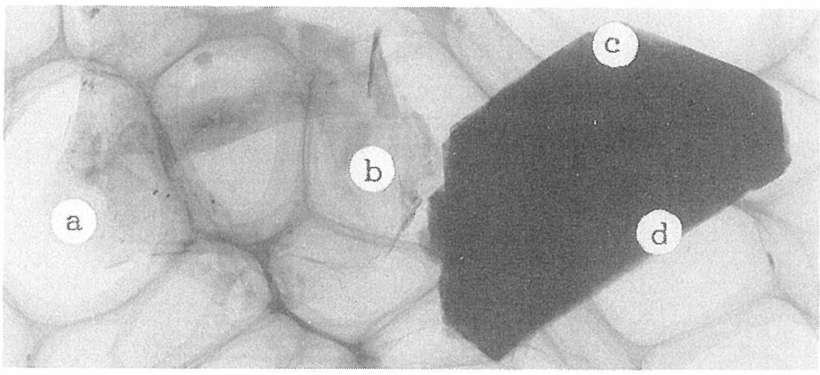

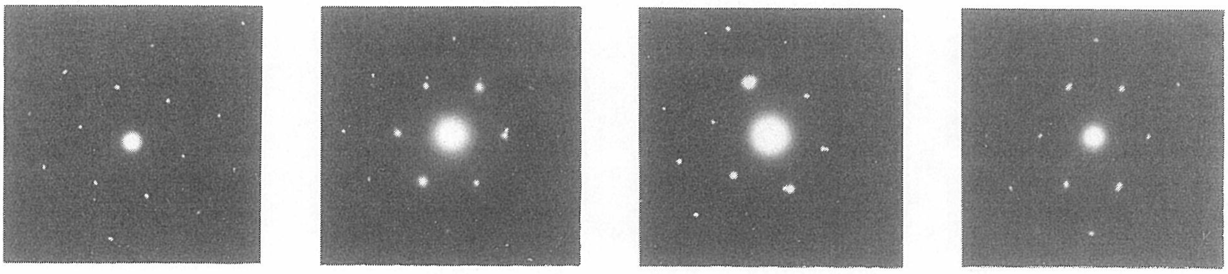

(4a) (4b) (4c) (4d)

diffraction patterns

SEM, 12KX

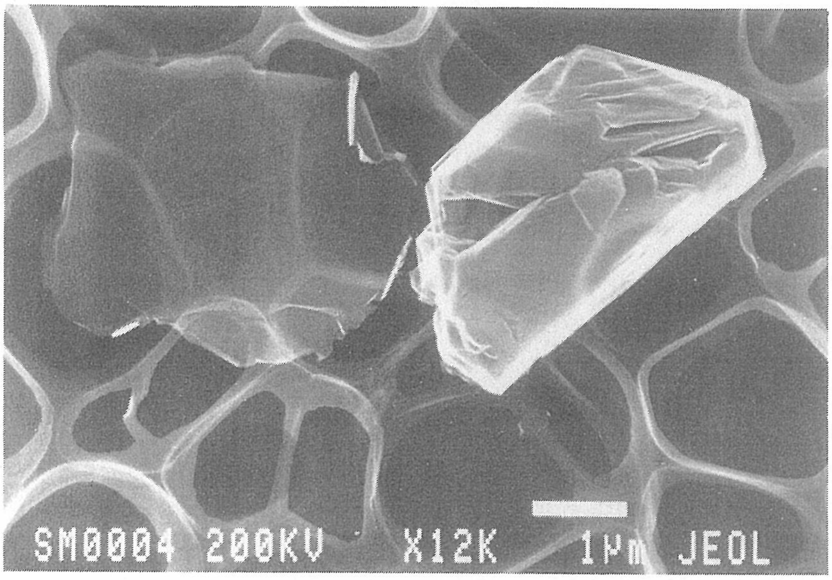

Fig. 4. Plain view of chunky graphite chips broken from chunky graphic cell and their diffraction patterns.

Segregation in Spheroidal Graphite Structure

The microstructure of analyzed specimen is shown in Figure 8 and the result of color mapping analysis on the spheroidal graphite structure is shown in Figure 9. The magnesium segregation was observed around all of the graphite nodules. This was a good example to explain the existence of Mg gas bubble as the site for spheroidal graphite.[1,2,13,21] As many researchers mentioned,[4,5] the negative segregation of Si was observed richly at the old austenite shells with graphite nodules and poorly among these austenite shells.

It was found that some spheroidal graphite had an inclusion in the graphite nodule, but most of the spheroidal graphite did not. They were mostly Mg-Ca-Si-S-O system inclusions. The morphology of these inclusions are shown in Figure 10. This will be considered later. Most of the inclusion existed at an area among the old austenite shell and consisted of Mg, Ce, Ca, Si, Ti, P, S, and O. An example is shown in Figure 11. These inclusions usually appear to be dark spots or microshrinkage with optical microscopy and bright spots with SEM, as shown in Figure 8.

Segregation in Chunky Graphite Structure

Since the average size of the chunky graphite cell was very big (approximately 0.8 mm^3), first, the chunky graphite structure was roughly analyzed at the wide area of 1.8x2.0 mm to get the relationship between the chunky graphite structure and the segregation.

The microstructure of analyzed specimen is shown in Figure 12. The segregation of C, Si, Mn, Ti, and N is shown in Figure 13. The Si segregation was weaker and the Mn segregation was stronger than that of spheroidal graphite structure. Ti was observed as TiN inclusion around the old austenite and some of them were connected to chunky graphite.

It was very hard to know the relationship between the chunky graphite structure and the segregated elements such as Mg, Ca, Ce, P, S, and O because of dark photos by the strong segregation. The segregation of these elements are illustrated in Figure 14.

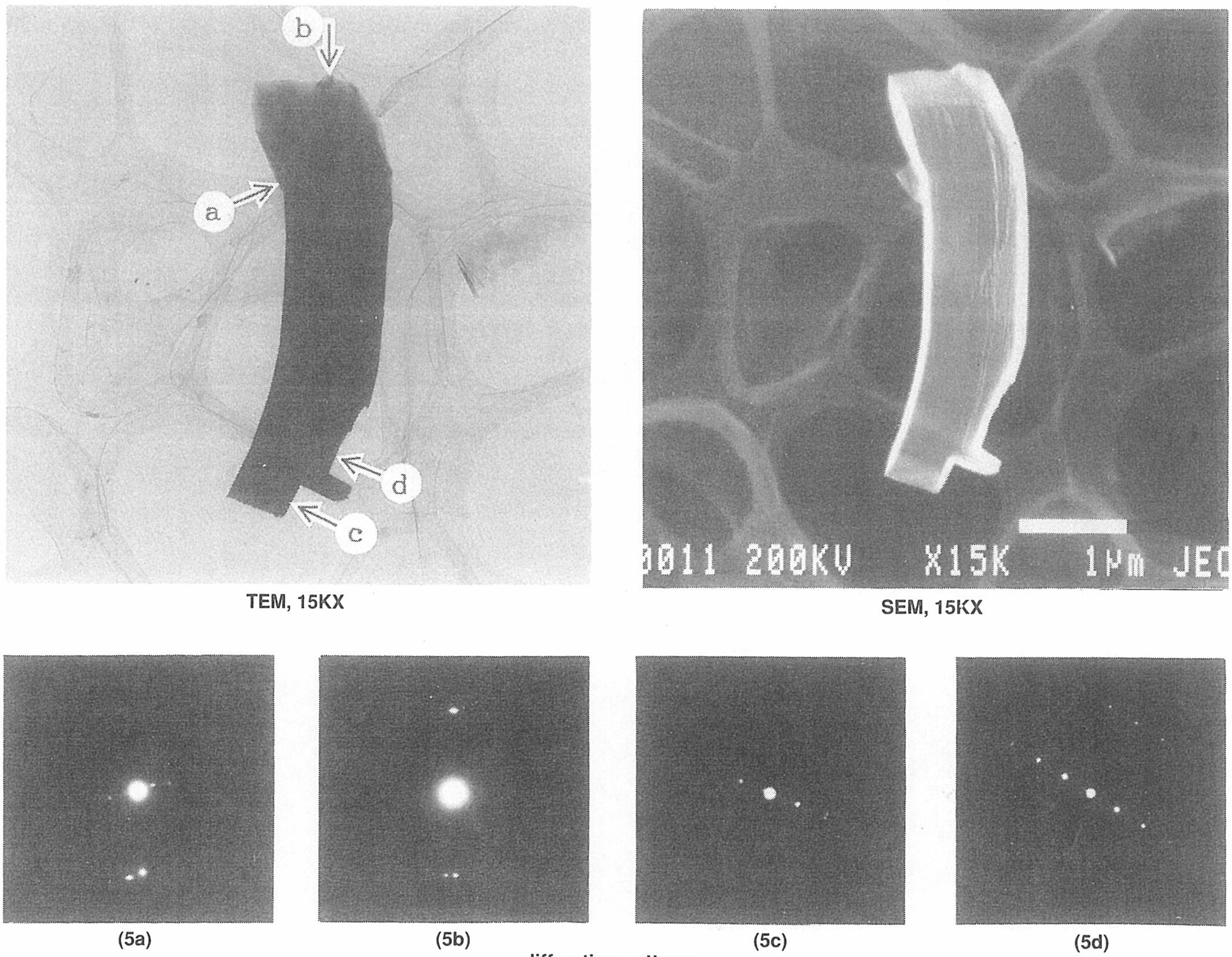

Fig. 5. Side view of graphite chips broken from chunky graphite cell and their diffraction patterns.

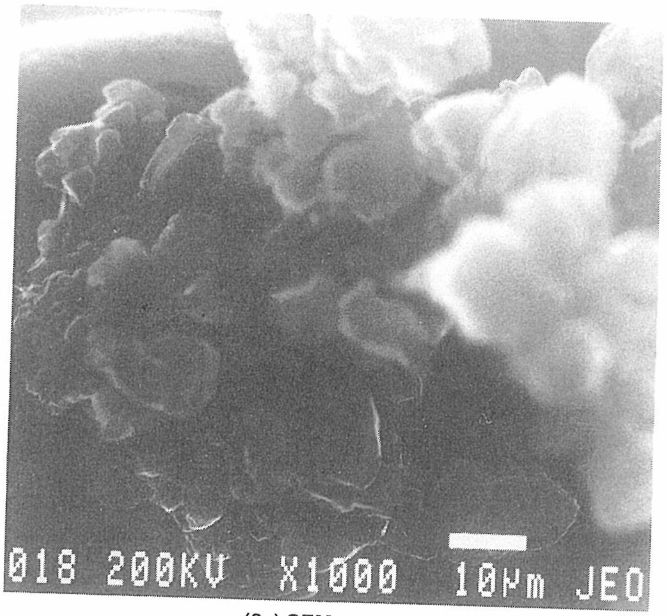

(6a) SEM, 1000X

(6b) SEM, 20KX

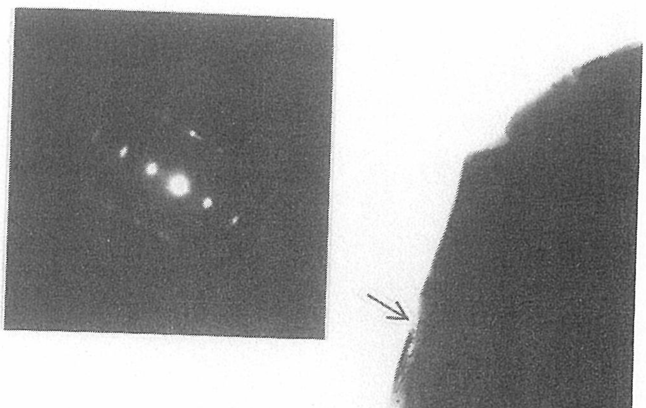

(6c) TEM (same view as photo b, 20KX) and diffraction pattern

Fig. 6. Chunky graphite cell and its diffraction pattern.

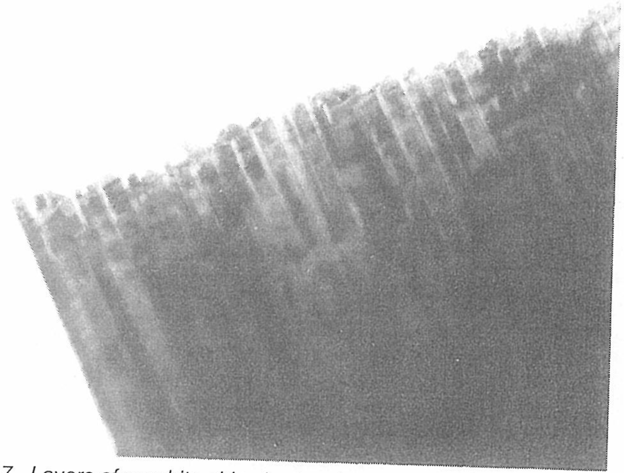

Fig. 7. Layers of graphite chips broken from chunky graphite cell (high magnification of Fig. 5, lower side) TEM. 100KX

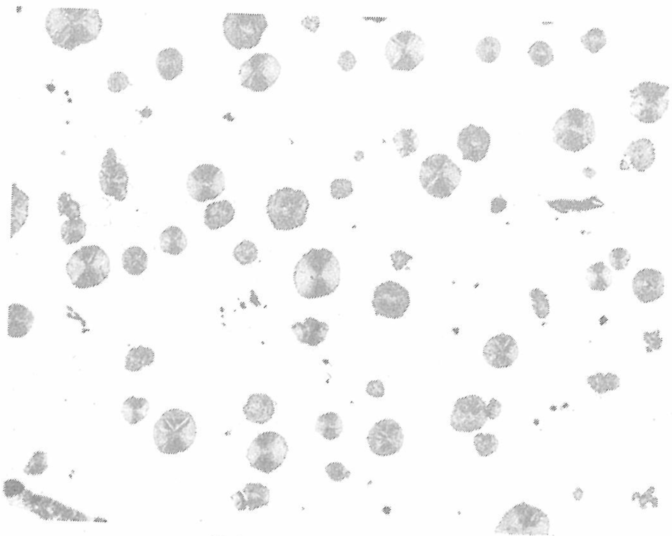

(8a) optical photo, 100X

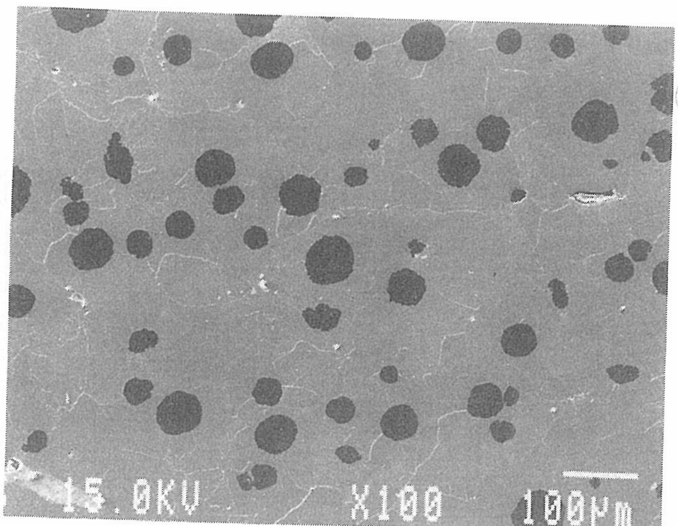

(8b) SEM, 100X

Fig. 8. Microstructure of spheroidal graphite specimen for color mapping analysis.

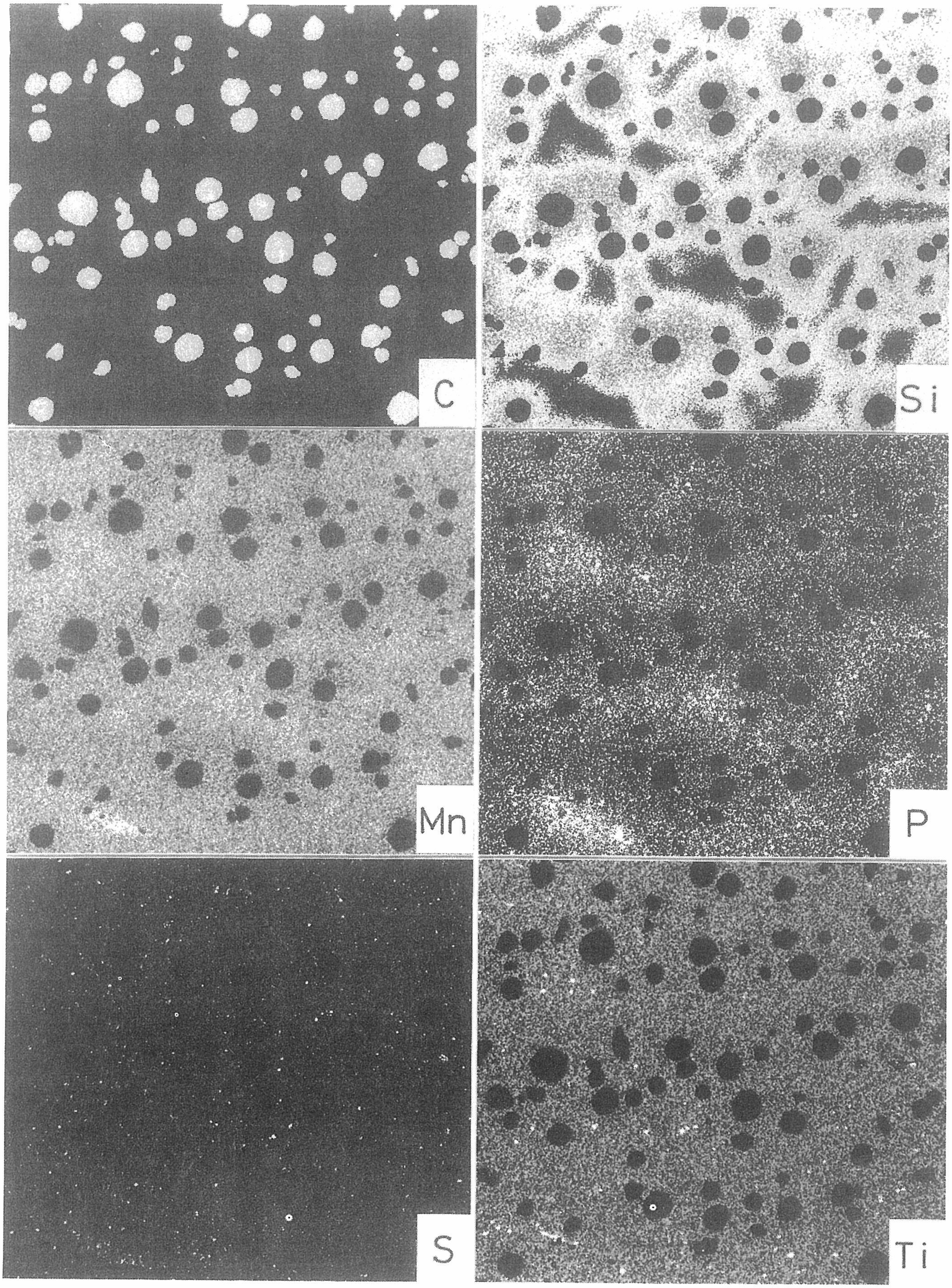

Fig. 9. Result of color mapping analysis for spheroidal graphite structure, mapping photo (90X). *(continued)*

Fig. 9 (continued).

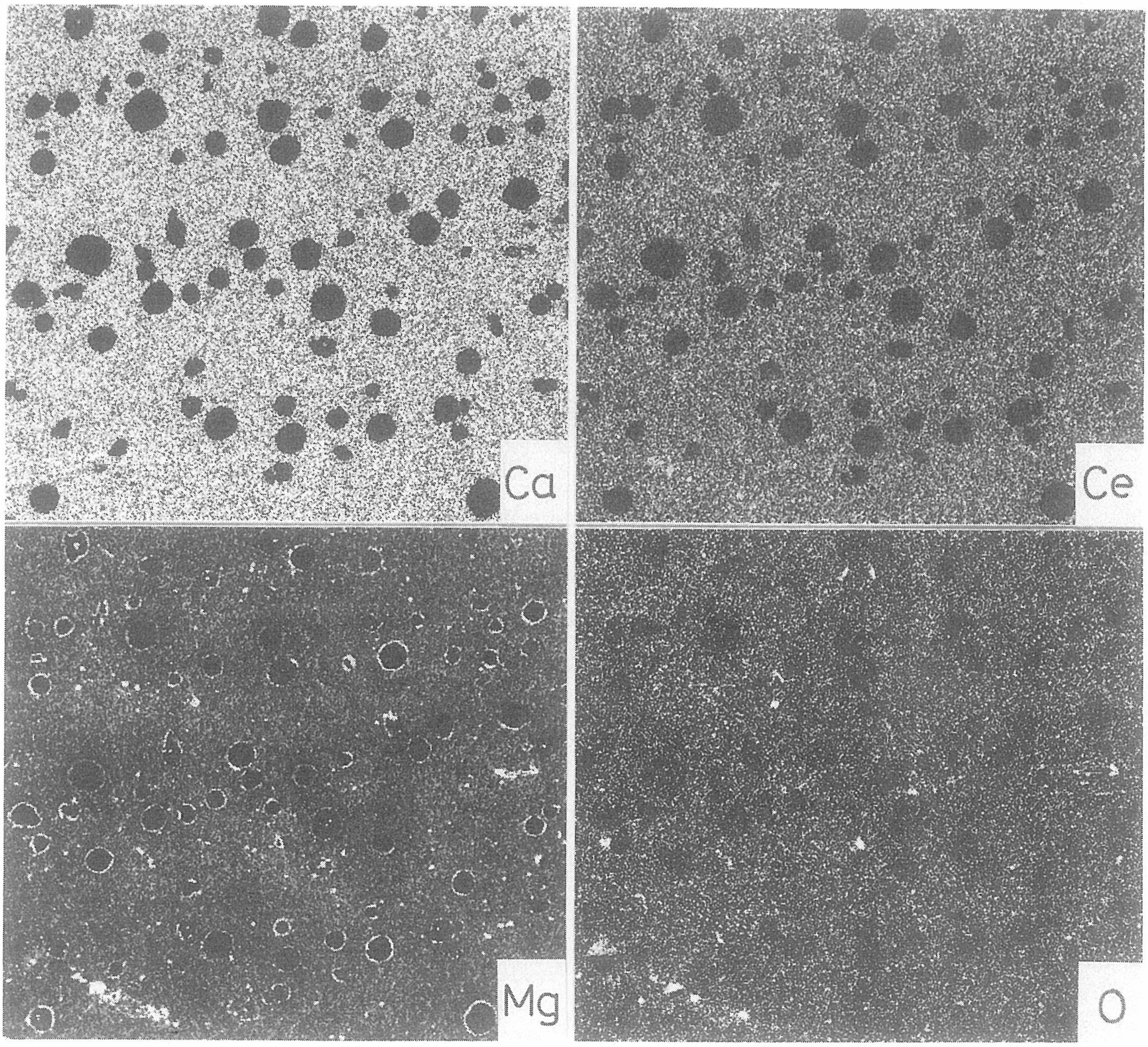

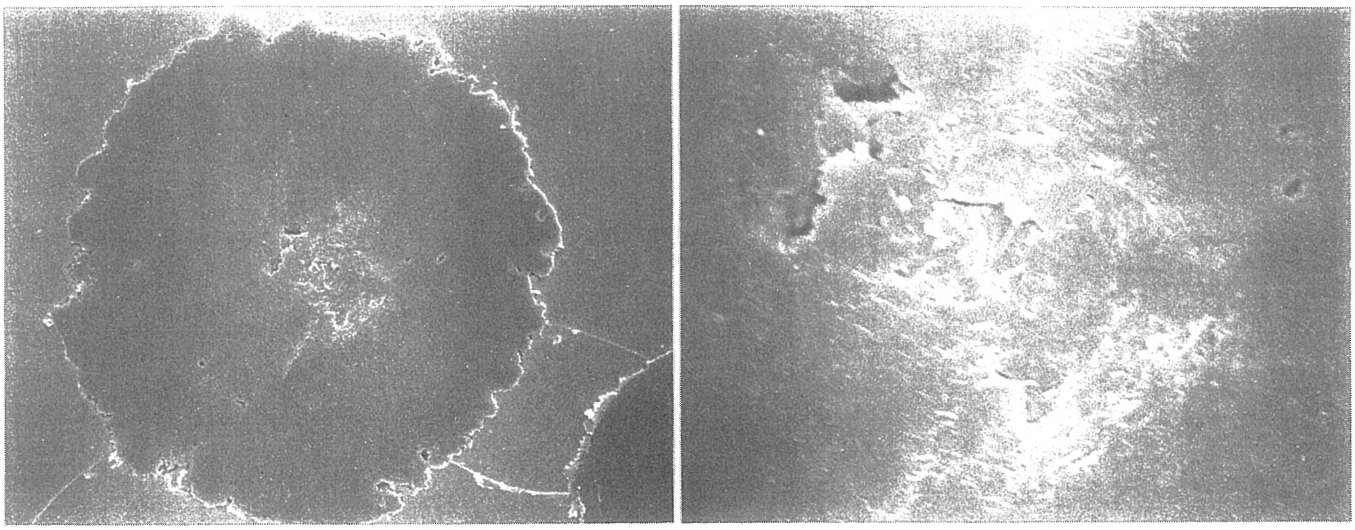

(10a) Mg-Ca-Si-S-O system, 1500X, 5000X

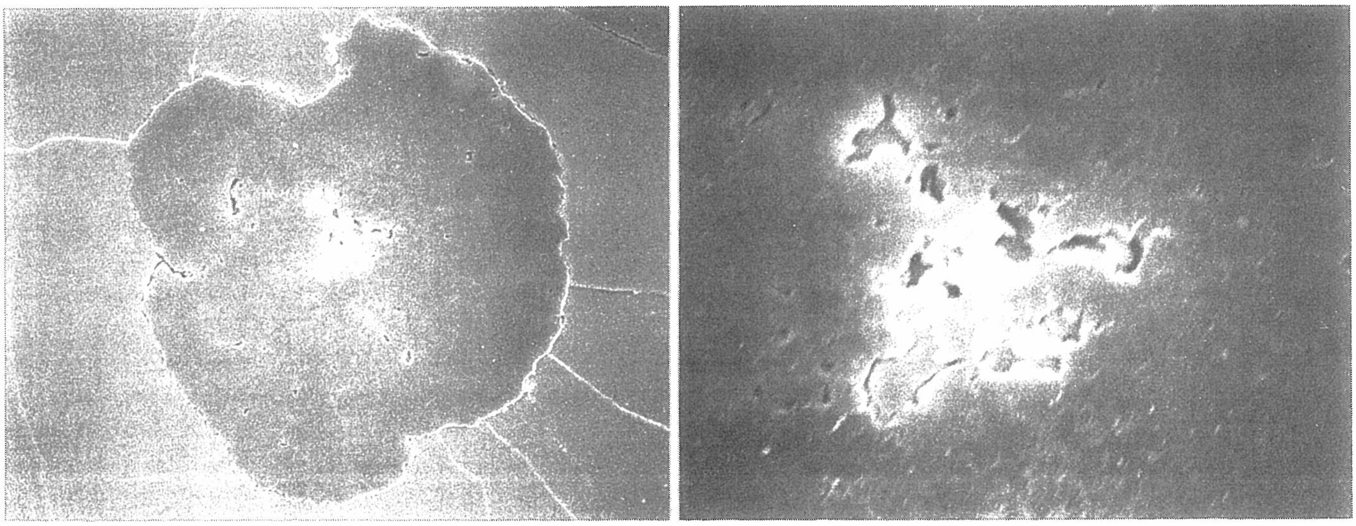

(10b) Mg-Si-S-O system, 1500X, 5000X

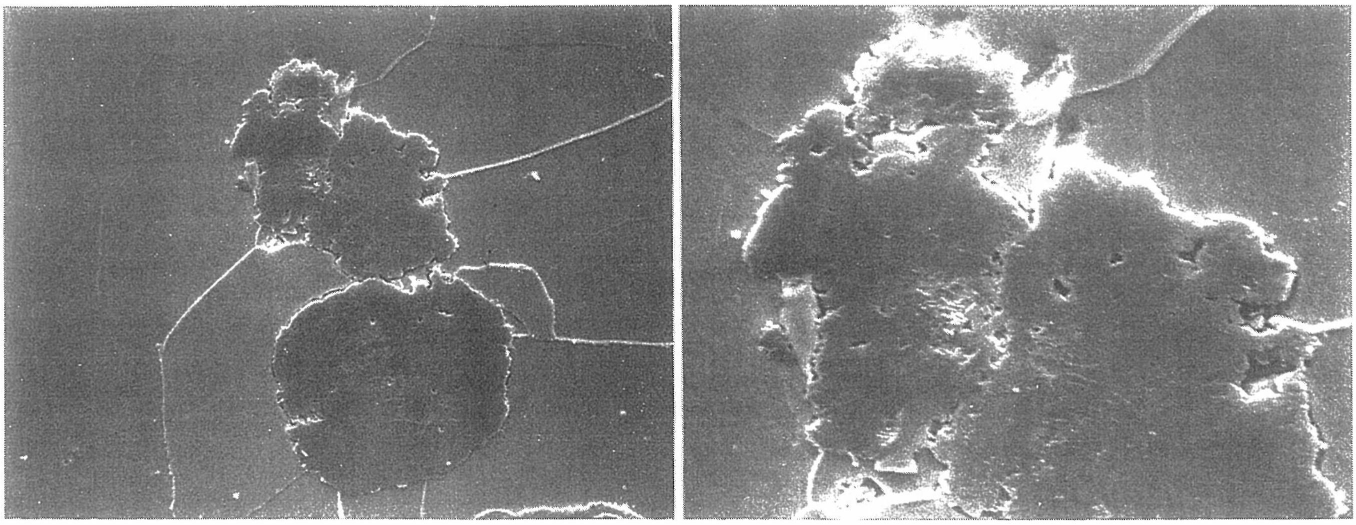

(10c) Mg-S-O system, 1200X, 2500X

Fig. 10. Inclusions in spheroidal graphite, SEM.

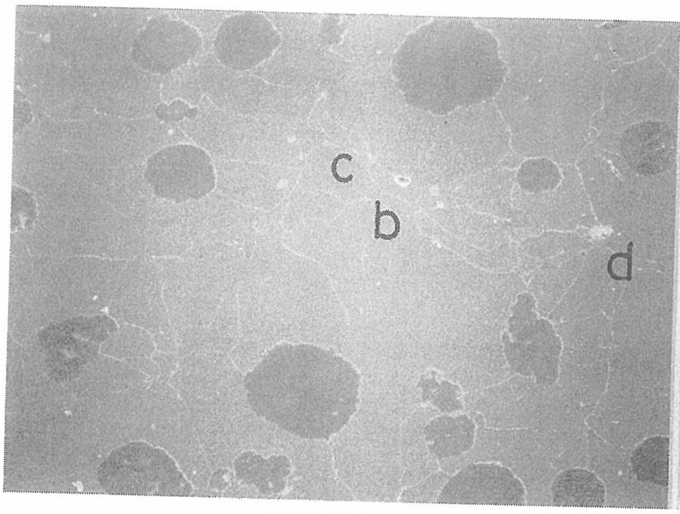

(11a) 250X

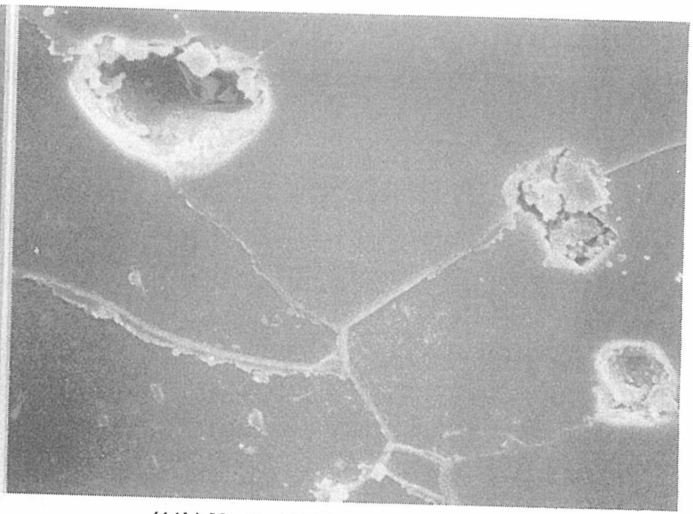

(11b) Mg-Ca-P-S-O system + TiN, 2500X

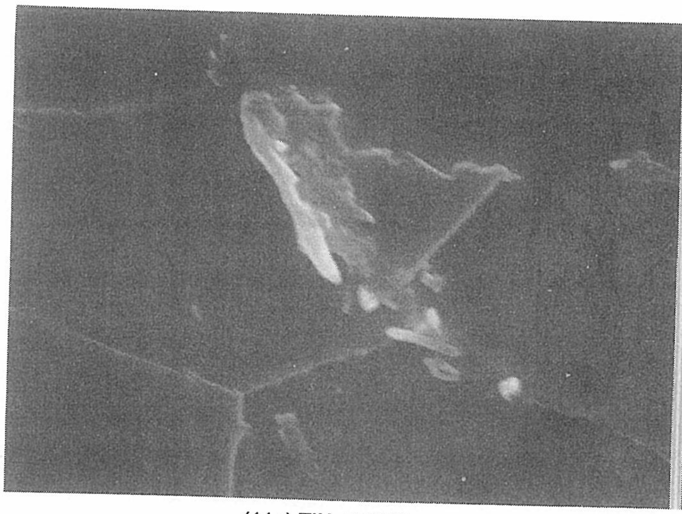

(11c) TiN, 7000X

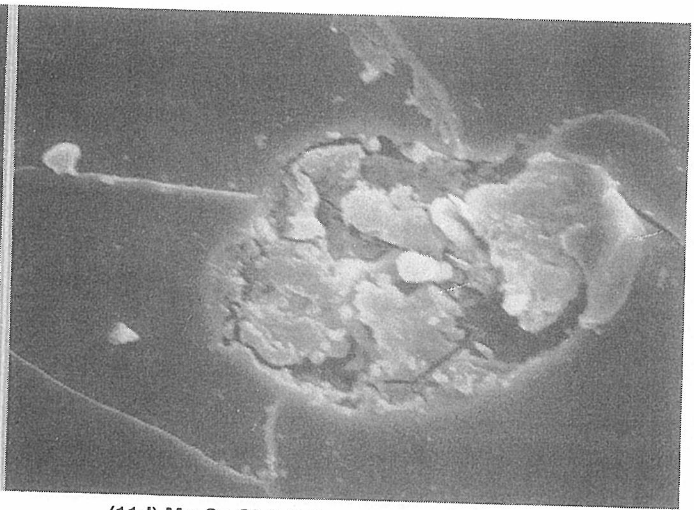

(11d) Mg-Ca-Si-P-S-O system + TiN, 5000X, SEM

Fig. 11. Inclusions at boundary of old austenite shell.

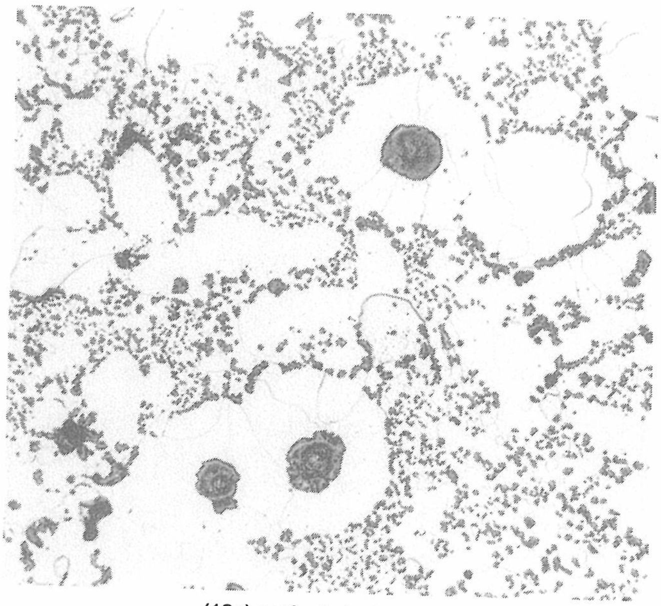

(12a) optical photo, 50X

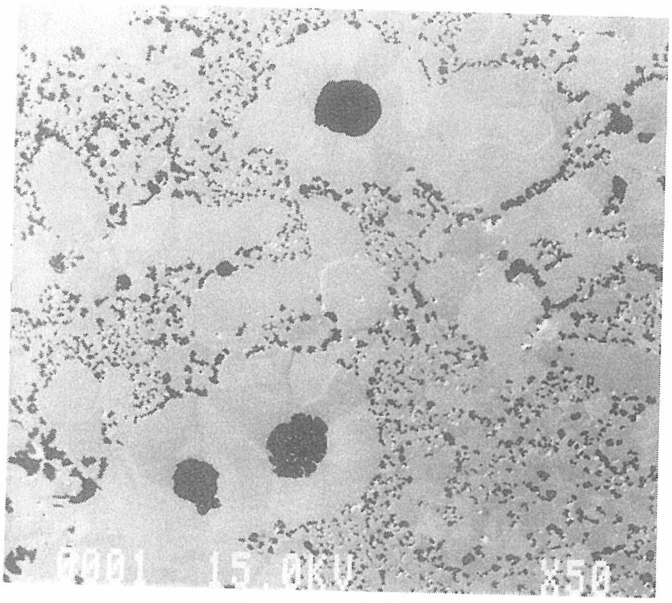

(12b) SEM, 50X

Fig. 12. Microstructure of chunky graphite specimen for rough color mapping analysis.

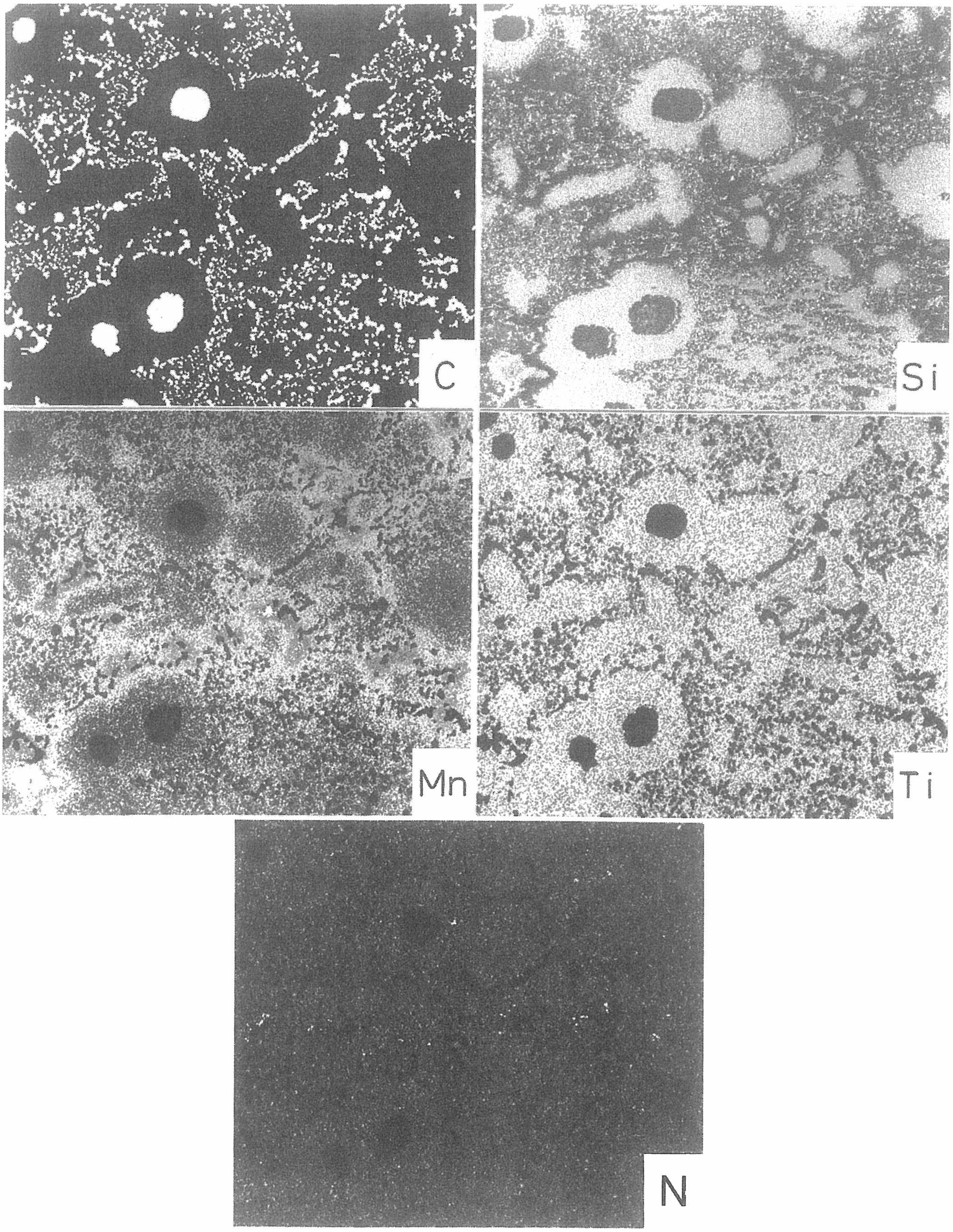

Fig. 13. Result of color mapping analysis for chunky graphite structure.

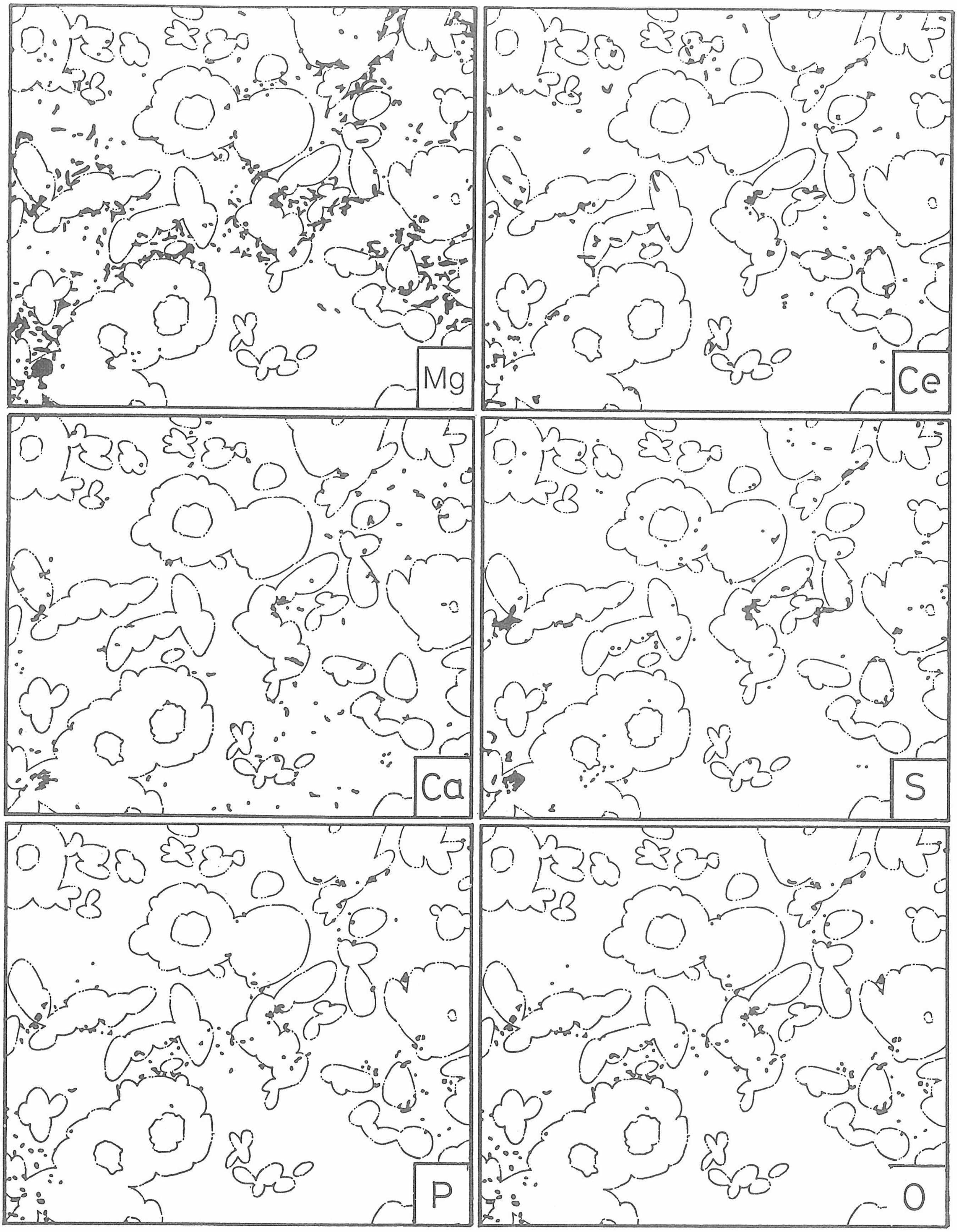

Fig. 14. Segregation of Mg, Ce, Ca, S, P, and O around old austenite in chunky graphite structure.

Yingyi[3] and Zhou[4] have reported that chunky graphite started to form at the austenite-residual melt interface at the middle stage of it after spheroidal graphite formed. Considering their results, the state at starting the chunky graphite formation appeared to be equal to an old austenite skeleton in Figure 12 and also almost same as highly rich Si area in Figure 13. The relationship between the old austenite skeleton and Si-rich area is shown in Figure 15. The segregation of other elements is illustrated on the structure of the old austenite skeleton, as shown in Figure 14.

Just like graphite nodules in the spheroidal graphite structure, Mg segregation was also observed around graphite nodules in the chunky graphite structure, although the segregation was not as dense as a common nodule. It was considered that this was the reason why

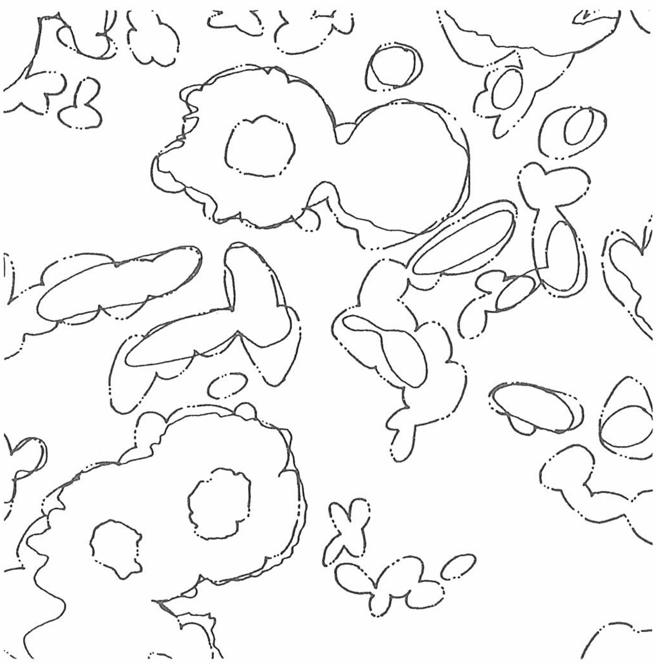

Fig. 15. Relationship between austenite skeleton and high Si area (100X).

spheroidal graphite in the chunky graphite structure was very big compared to that in Figure 8. Therefore, Mg density in austenite shell around graphite nodules would be sparse. The concentration of Mg, Ca, Ce, P, S, and O was observed between the old austenite shell and dendrite and between the old austenite dendrites. A similar result was reported by Yingyi[3] that there was the concentration of RE, Mg, S, and O at solidification front of chunky graphite. They added that the segregation of Ca, Y, Ce, at the chunky graphite area was higher than that at the spheroidal graphite area. The result in this study, however, showed that this segregation was not in every chunky graphite area but in the above site.

The segregation tendency could be known as above. Therefore, the relationship between the segregation elements and the initial precipitation site for chunky graphite was observed in detail as next step. The microstructure of analyzed specimen is shown in Figure 16. The same elements observed in the strong segregation against the chunky graphite structure in Figure 14 will be explained here. The segregation of those elements was illustrated on the chunky graphite structure and the result is shown in Figure 17.

Mg was observed as a metallic state and inclusions at the initial precipitation site for chunky graphite. An example of Mg segregation between the old austenite dendrites (left upper corner in Fig. 17) is shown in Figure 18. Another example of Mg segregation at the old austenite shell-chunky graphite area interface (center in Fig. 17) is shown in Figure 19. Si, Ce, S, P, and O were also observed in these sites in Figures 18 and 19. Although it is quite a small quantity, Al was observed at inclusion in Figure 19. Some microshrinkage at or around inclusions were observed.

Another type of inclusion was observed in chunky graphite cell and shown in Figure 20. This type of inclusion was analyzed with EDAX and the result is shown in Figure 21. Since Fe-Ca and Al-Ca metallic inclusions are chemically impossible, this may be a oxide inclusion or oxide-nitride dual inclusion.

Thus, metallic Mg and some kind of inclusion might be considered as kinds of the initial precipitation sites for the chunky graphite formation. Metallic Mg was considered as a liquid state at the eutectic reaction range, and will be discussed later.

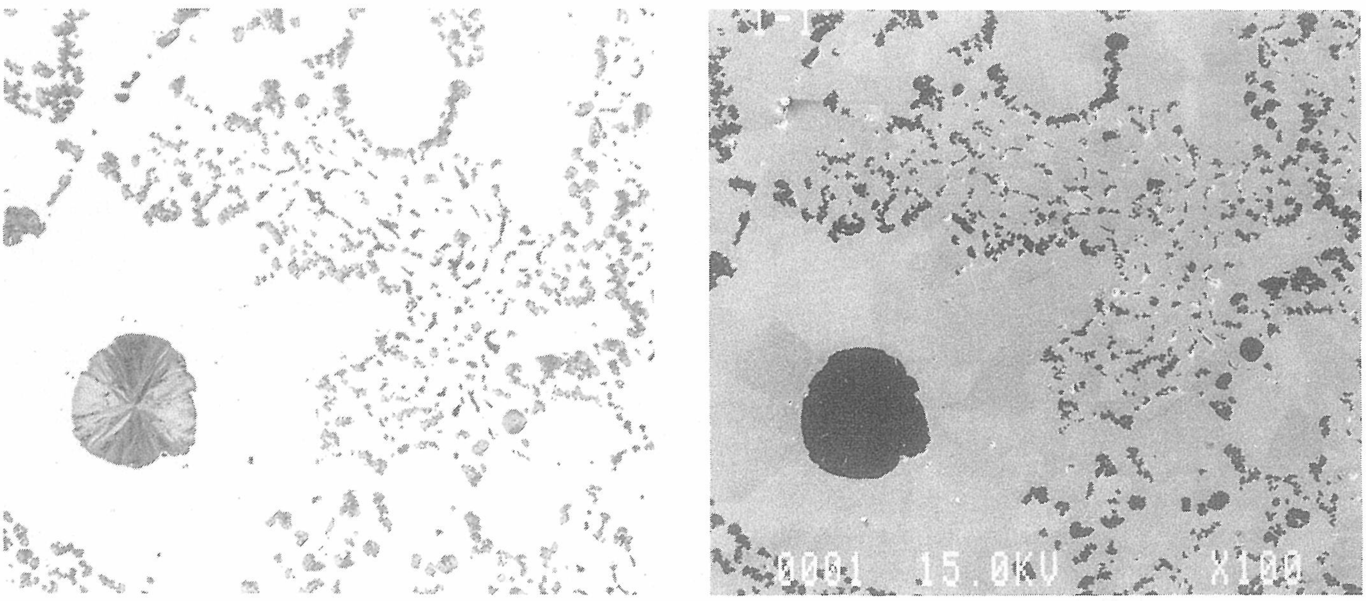

(16a) optical photo, 100X **(16b) SEM, 100X**

Fig. 16. Microstructure of chunky graphite specimen for detail color mapping analysis.

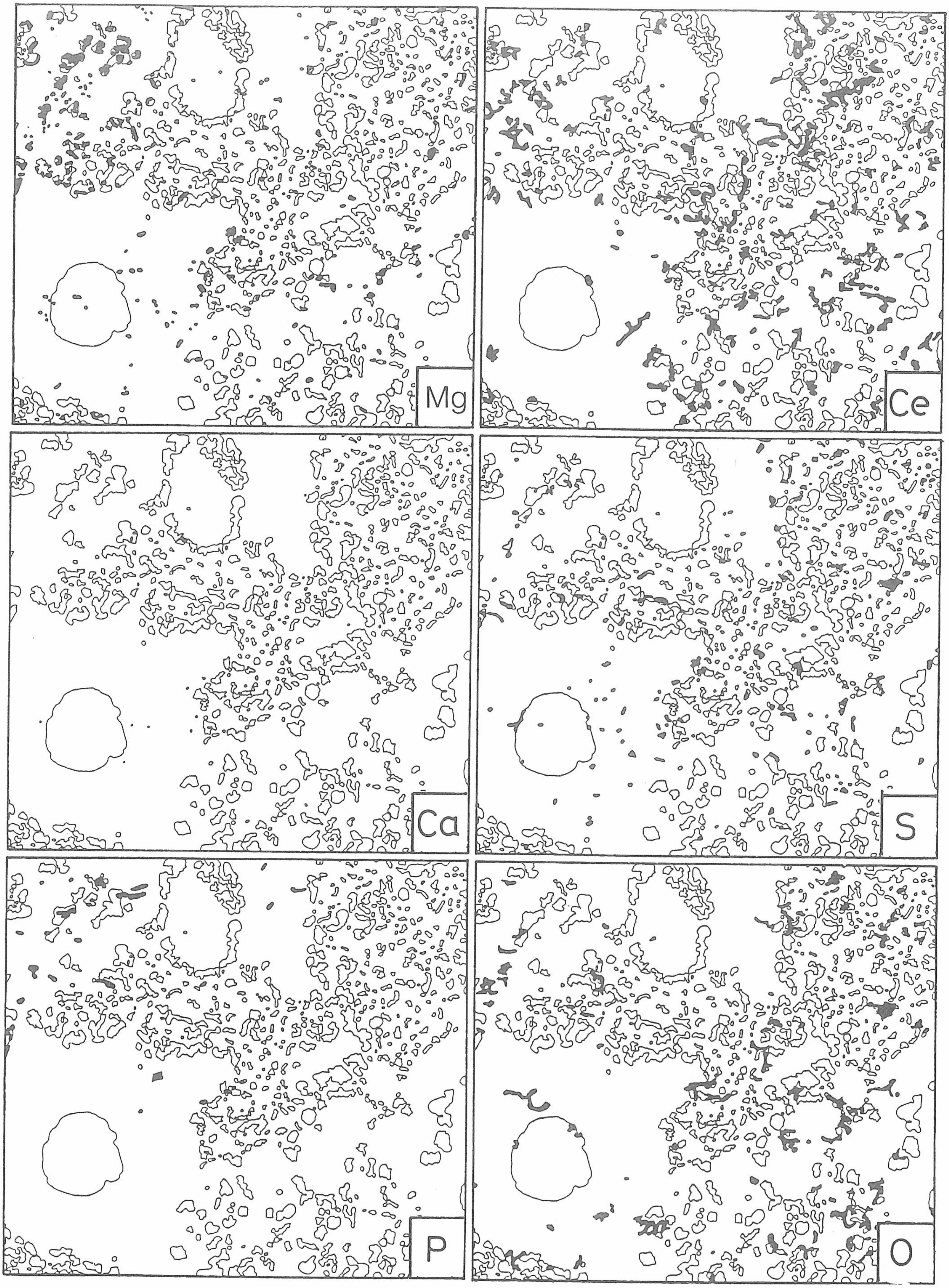

Fig. 17. Segregation of Mg, Ce, Ca, S, P, and O at initial site for chunky graphite formation.

CONSIDERATION

Formation Mechanism Considered from the Substructure

In former studies,[1,2] it was concluded that the graphite-precipitated site had an important key for the graphite substructure. In order to be CV and spheroidal graphite, the site limiting the dominant a-axis growth of hexagonal graphite crystal was needed, such as the bubble introduced by spheroidizer, the interface between spheroidal graphite and austenite shell, and the thin melt channel connected between the graphite end and residual melt in the austenite shell.

Since it was found in this study that the substructure of chunky graphite was basically the same as those of CV and spheroidal graphite, chunky graphite might take the same formation as them.

According to Yingyi[3] and Zhou,[4] the chunky graphite formation process was considered as follows:

1) *At the early stage of the solidification,* graphite is precipitated as spheroidal graphite and it is surrounded by austenite shell.
2) *At the middle stage of the solidification,* the spheroidal graphite nucleation finished and the chunky graphite started to precipitate at the austenite-residual melt interface.
3) *During the growth of chunky graphite,* the end of chunky graphite is contacted with the residual melt through the thin melt channel.

Thus chunky graphite is a quite similar formation process to CV graphite. The difference is that chunky graphite is not likely to be connected with spheroidal graphite during the growth, but CV graphite is. The most important thing in common term to chunky and CV graphite is that graphite is precipitated at the thin melt channel in the austenite shell. This is the reason these graphites basically possess the same substructure and the similar appearance.

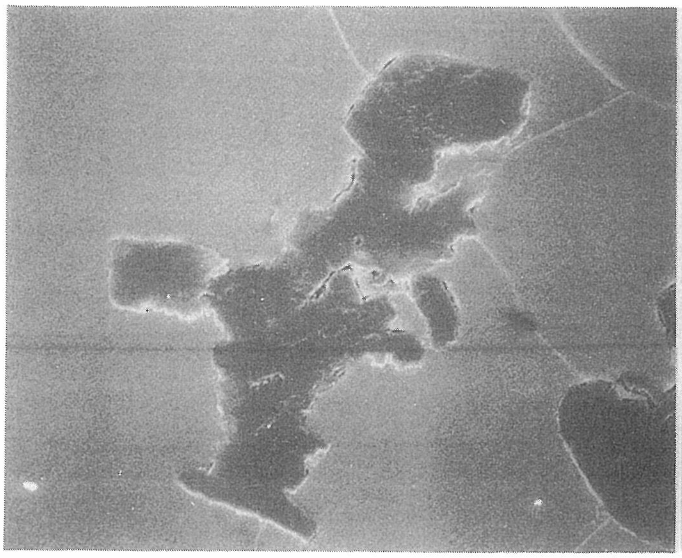

(18a) 3000 X

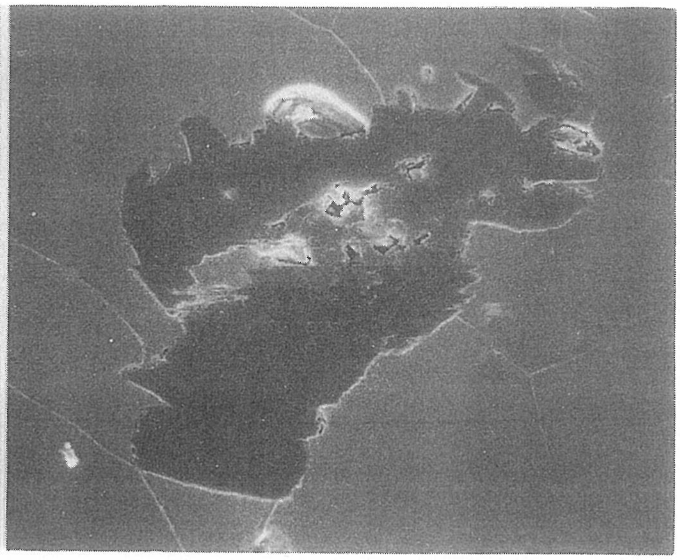

(18b) 3000X

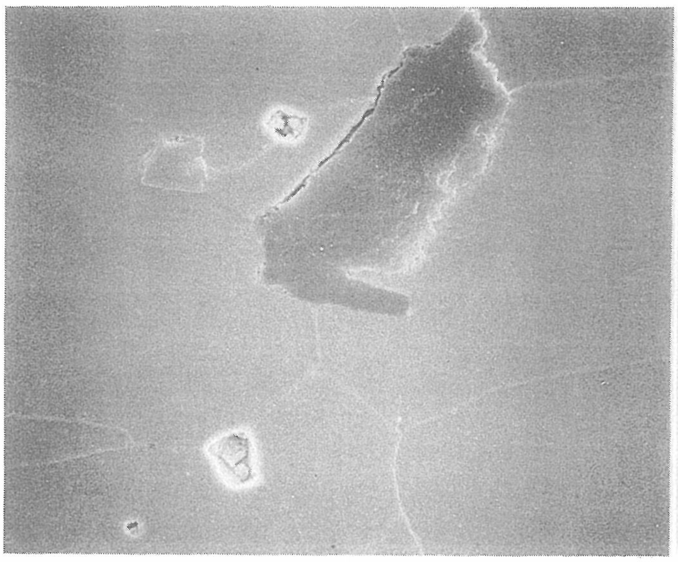

(18c) 2500 X

(18d)

Fig. 18. Mg segregated area and chunky graphite structure between old austenite dendrite.

Liu[6] and Zhou[4] have reported that chunky graphite takes the manner of the spiral or screw dislocation growth the same as spheroidal graphite. It will, however, be impossible for the graphite formation to keep such a dislocation throughout the whole graphite formation, because it is the only defect of graphite crystal and no one may command carbon atoms to do so. A diffusion of carbon atoms would be always faster than that of iron atoms, even if the state was a liquid or solid phase. This means that the graphite formation is always dependant on the diffusion of iron atoms.

The carbon atoms may naturally be bonded as graphite by the principle of hexagonal graphite crystal. As the result of this study, it was actually found that chunky graphite was composed of graphite chips and that, although the spiral-like growth was observed at some graphite ends, it was not the manner of the whole growth for chunky graphite.

Formation Mechanism Considered from Segregation

Yamamoto, Chang,[13,21] and others[1,2] have reported that gas bubbles act as the initial nucleation site for spheroidal graphite. It was proved further in this study that Mg segregation was clearly observed at austenite shell around all of the graphite nodules in the spheroidal graphite structure and even around graphite nodules in the chunky graphite structure. There was no Mg segregation around each chunky graphite, but Mg was segregated on some chunky graphite between austenite dendrites and between austenite shell and dendrite. That is to say, Mg segregated around the old austenite. As the cause of the chunky graphite formation, it was considered that the heavy section and long solidification brought a lack of Mg as the nucleation site for spheroidal graphite, a homogeneous distribution of Si and a concentration Mg, Ce, P, S, O, etc., at the austenite-residual melt interface before chunky graphite started to precipitate, and that elements promoting chunky graphite precipitation such as Ce, Ca, Si, and Ni helped these phenomena. Each cause is explained in detail as follows:

Lack of free surface for spheroidal graphite formation. This means the lack of available Mg in the melt for spheroidal graphite. It is considered that the available Mg may disappear by a second oxidation during pouring, reaction with refractory,[12] fading out from the melt by the floating of gas bubbles,[13] and metallic Mg segregation at austenite-residual melt interface.[13]

In the above case, Mg segregation is considered the most effective reason for the chunky graphite precipitation. Yamamoto et al.[13] have reported that graphite nodules were reduced in number and deteriorated in shape into mesh-like graphite when the melt was solidified under higher pressure than the equilibrium vapor pressure. They added that, in the melt, Mg became harder to be in the gas state by boiling up and existed as the liquid droplet when the melt was exposed over a certain

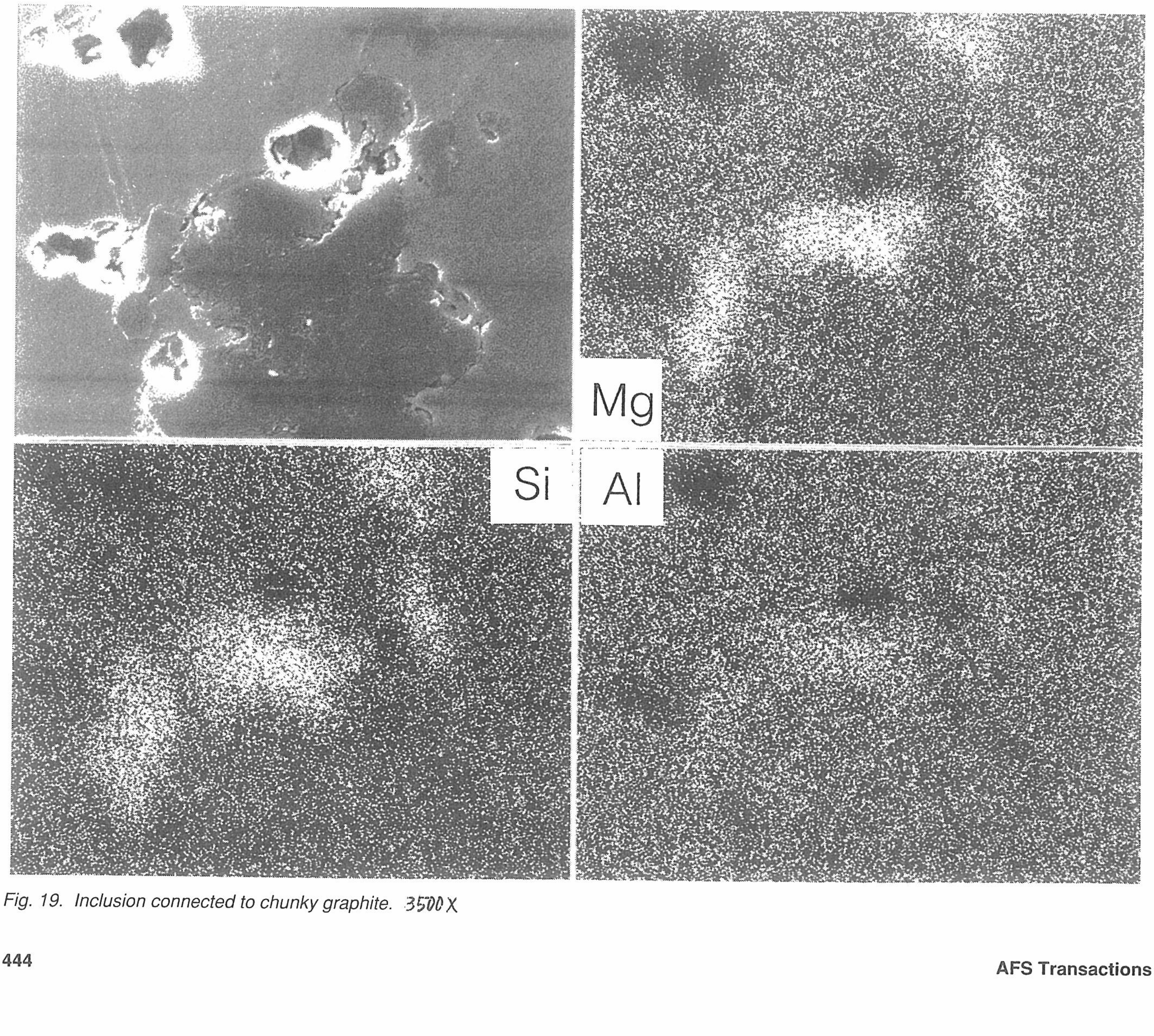

Fig. 19. Inclusion connected to chunky graphite. 3500X

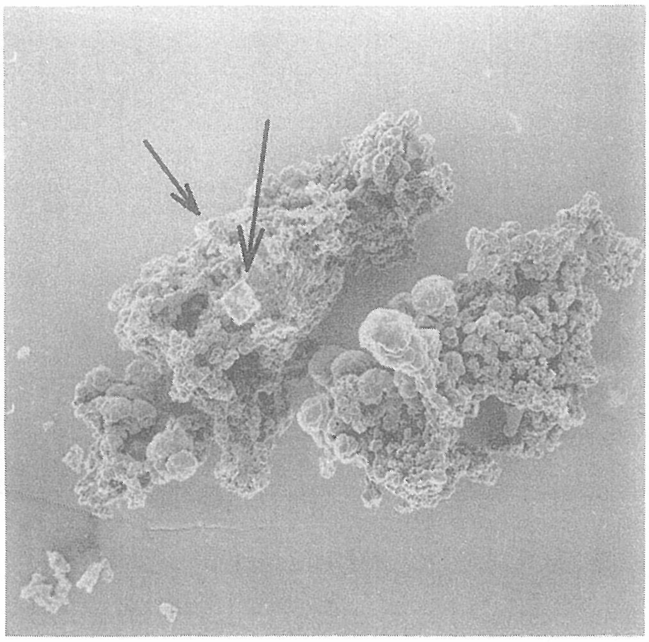

(20a) . 50X

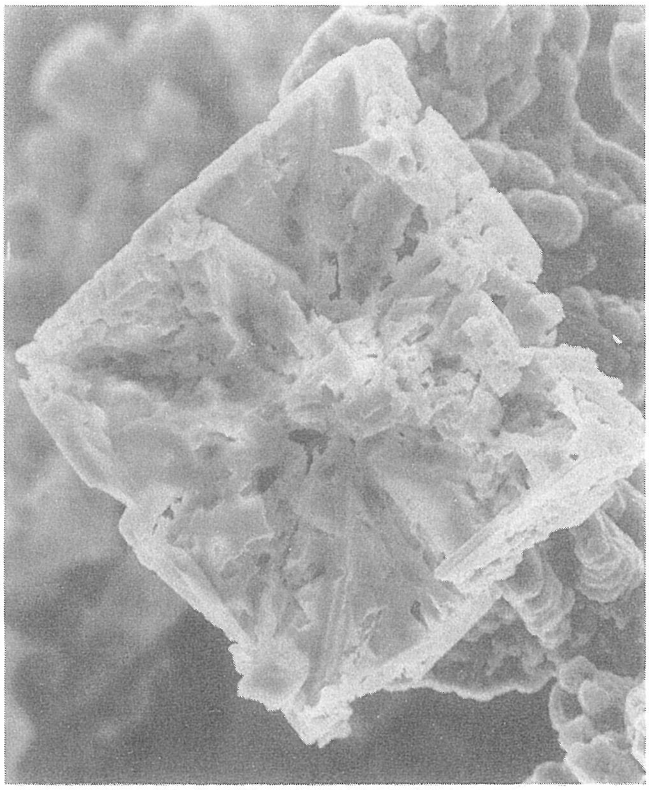

(20b) 750 X

Fig. 20. Inclusions in chunky graphite cell.

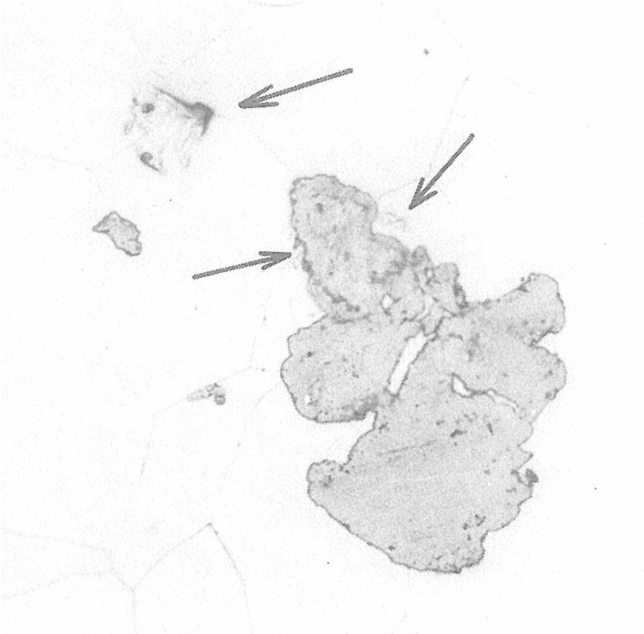

(20c) 400 X

pressure, before and during solidification and, therefore, the Mg bubble as the site for spheroidal graphite formation was decreased in the residual melt. It seemed that graphite was not recognized as chunky graphite at that time. The nodule deterioration (Figs. 1 and 12) and Mg segregation (Figs. 14 and 17) in this study were similar phenomena to their result. Therefore, it was considered that the chunky graphite formation at the thermal center in heavy-section ductile cast iron might occur when the melt was solidified under higher pressure than the equilibrium vapor pressure of Mg at the solidification temperature and a lack of Mg gas bubble as free surface. In this case, the liquid Mg-melt or austenite interface might be considered as the nucleation site for chunky graphite, if carbon was enriched around there and graphitization were easier than spheroidal graphite-austenite shell interface.

The thermal center may receive some eutectic expansion pressure from the first solidified surface layer before the solidification start. According to Yamamoto,[13] the critical pressure is a few atoms at near-solidification temperature. On the other hand, the eutectic expansion has reported 50–60 atoms in eutectic composition.[26] Even if the whole pressure did not work toward the inside (because of the shrinkage compensation and swelling), if the thermal center delayed enough to start the solidification of the surface layer, some of the pressure might work for the chunky graphite formation.

It is very important for the chunky graphite substructure to be surrounded with austenite after the nucleation and to contact with residual melt through thin melt channel. This is a similar phenomena as the CV graphite formation.

The site between austenite dendrites and between austenite shell and dendrite might also act as the nucleation site for chunky graphite.

Homogeneity of Si distribution. Si was homogenized in the chunky graphite structure by long solidification. This may also help a small number of the spheroidal graphite nucleation.

Role of elements promoted chunky graphite formation. Karsay[10] has reported that the chunky graphite precipitation was promoted by the content or addition of Ce, Ca, Si, and Ni. It was considered that high Ce, Ca, Si, and Ni made the eutectic reaction range open according to many researchers[14,19] and made the solidification time longer, and that it helped to reduce the free site for spheroidal graphite and to promote chunky graphite precipitation as mentioned above. Ce was also considered as a stabilizer of the thin melt channel for chunky graphite.

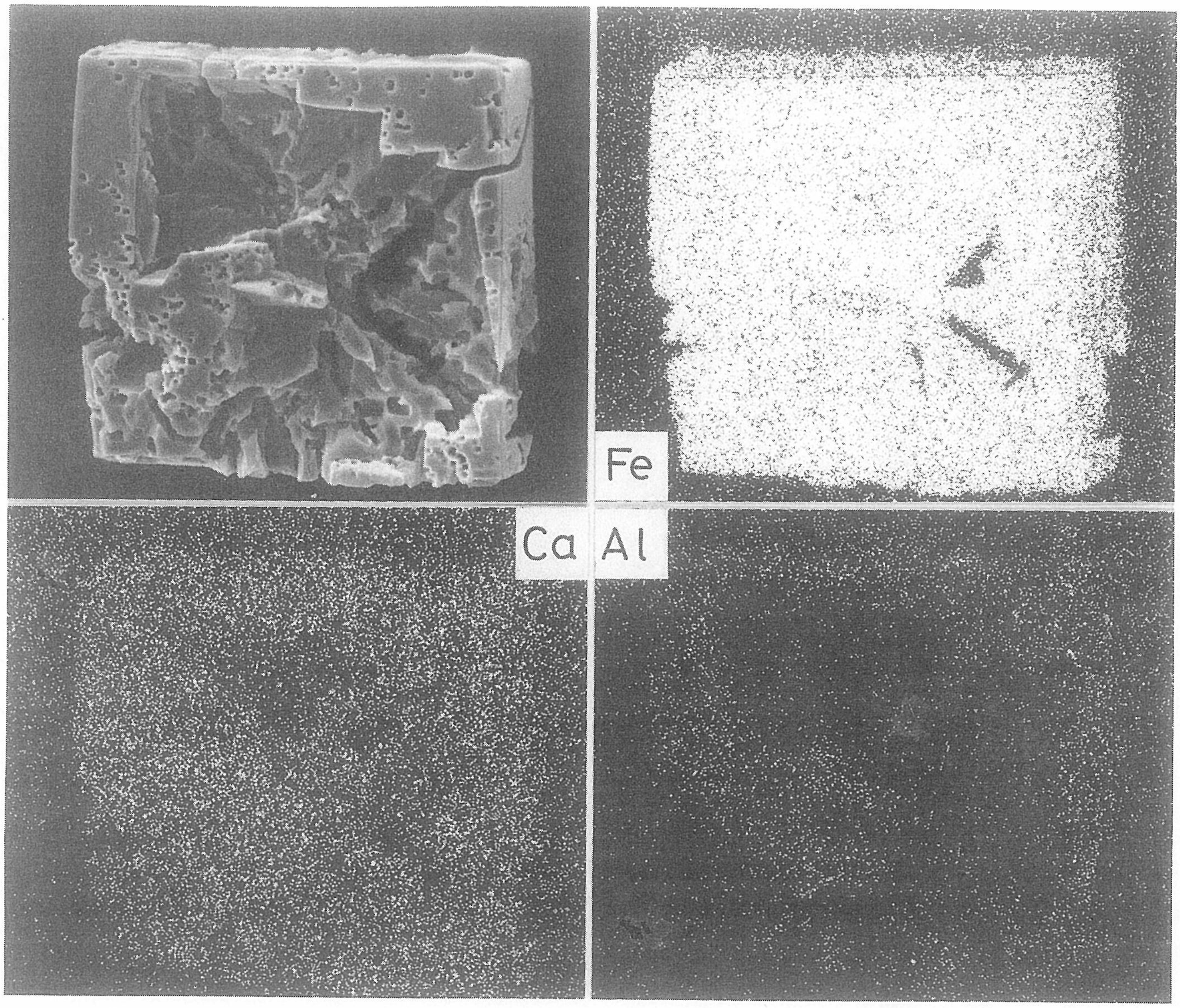

Fig. 21. One of inclusions extracted from chunky graphite specimen, SEM (l000X).

Role of inclusion. Although some inclusions were observed in the spheroidal graphite (as already argued), the inclusion was not considered as nuclei for spheroidal graphite. This was already proved by Pohl[20] and Yamamoto.[13,21] Even if graphite was precipitated at the surface of the inclusion, there might be no reason why the inclusion had commanded graphite or carbon atoms to become spheroidal graphite during the whole formation process. That is to say, inclusion might have no DNA (deoxyribonucleic acid in biology). It was considered that the inclusion was trapped by the gas bubble and graphite was precipitated at free surface just like a normal gas bubble and that it caused some spheroidal graphite with inclusion, as shown in Figure 22.

However, there might be some possibility for irregular graphite, like chunky graphite, to begin a nucleation from inclusion. For example, if inclusion existed at a carbon-rich area, graphite would precipitate at melt-inclusion interface. The most important term to become polycrystal graphite, like chunky graphite, will be that the graphite around the inclusion should be surrounded with austenite shell soon after graphite begins to precipitate, and that the graphite end should be connected with residual melt through a thin melt channel. That is to say, the inclusion may not be very important for chunky graphite growth and give only first nucleation site but the thin melt channel connecting the residual melt and graphite end in austenite shell may be very important.

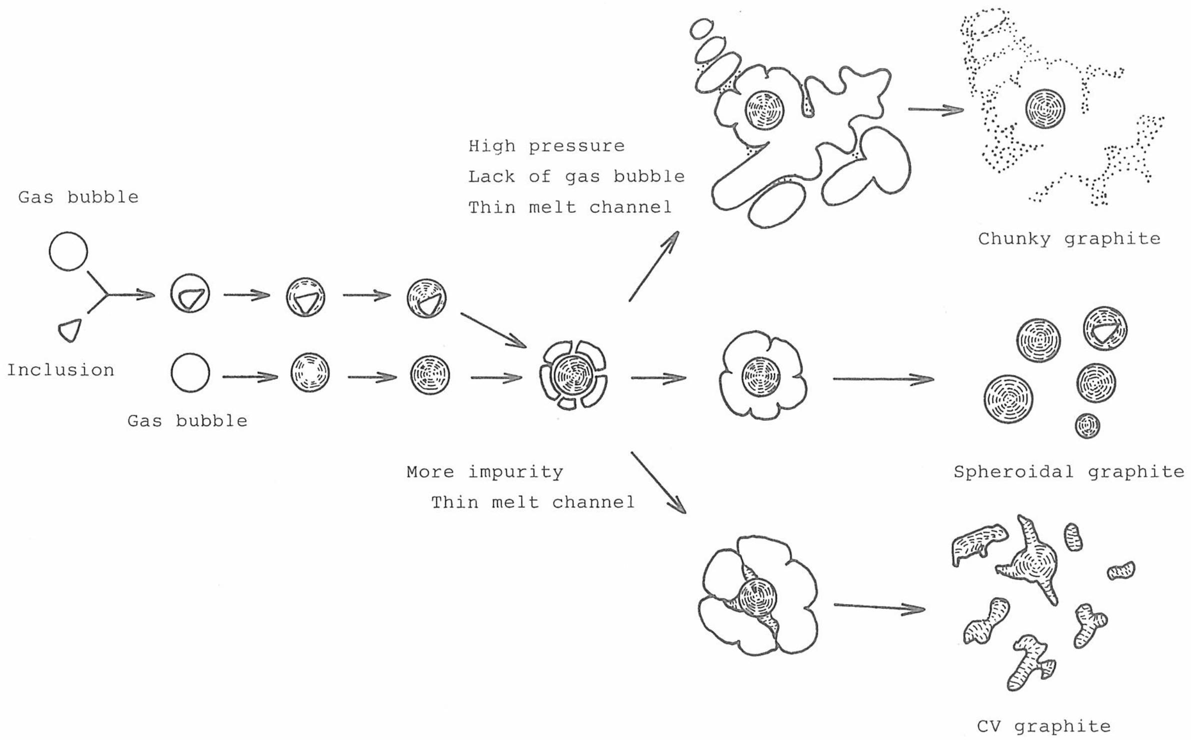

Fig. 22. Schematic illustration of graphite formation in molten iron treated with spheroidizer.

Chunky Graphite Formation Mechanism

The chunky graphite formation mechanism in heavy-section ductile cast irons was considered as shown in Figure 22 and explained as follows:

1) The thermal center (precipitated chunky graphite) is delayed to solidify more than the surface layer.
2) The thermal center may receive the pressure of eutectic expansion from the surface layer and, therefore, Mg gas bubble may fade out from there before the solidification starts.
3) Small numbers of Mg gas bubbles can exist in the melt under such a circumstance and graphite precipitates into them as spheroidal graphite at the early stage of the solidification.
4) Liquid Mg, caused by the pressure of eutectic expansion, segregates at austenite shell or dendrite-residual melt interface.
5) After spheroidal graphite precipitates, chunky graphite starts to precipitate at interface among liquid Mg, austenite shell and dendrite, inclusion, residual melt, etc., at the middle stage of the solidification.
6) During growth, chunky graphite ends contact with residual melt through the thin melt channel.

Proposal of Site Theory

Before the chunky graphite formation mechanism was known, this theory was only an idea.[1,2] But, since it was cleared at this study, the site theory was introduced here. It was found that all types of the graphite formation mechanisms in cast irons could be explained by this theory.

Although some patterns of structural defects (like a screw dislocation) are observed in graphite crystal, the basic behavior of graphite growth may never be changed, as dominantly grown along the a-axis and subordinately grown along the c-axis of the hexagonal graphite structure. In new theory, it was defined that the graphite morphology might be dependent on the site where graphite precipitated. That is to say, graphite does not take morphology by itself but graphite is given the morphology by the site and graphite grows along the site.

If graphite—before and during the growth—was given no restriction as the site in the melt, graphite would grow as the most stable state of kish graphite. If graphite—before and during the growth—was given the restrictive site, but did not disturb the dominant growth of a-axis, graphite would grow as flake graphite. If graphite—before and during the growth—was given a free site or semi-free site such as gas bubble in the melt, graphite-austenite interface and the thin melt channel in austenite, graphite would grow as spheroidal graphite, etc. In those free sites at austenite, graphite can grow when the atoms of the elements composed of cast iron diffuse at the graphite-austenite interface and the site becomes bigger because the diffusion of iron atom is much slower than that of carbon atom in both liquid and solid phase, for example.

Since graphite is an excess object of cast iron, and basically grows along the a-axis of the hexagonal graphite crystal, it never bonds with the other elements in cast iron. The fundamental behavior of the nucleation and growth might be basically the same among graphites, even if the state was different, like the liquid or solid phase.

Lee[22,23] and Hanawa[24] have reported that the morphology of temper graphite was just dependent on the morphology of the void where graphite precipitated. According to their theory, the morphology of temper graphite could be controlled by controlling the morphology of the void and was dependent on a diffusion of atoms in cast iron when graphite grew bigger than the initial void. Kawano[25] has also reported that a sharp end of D-type graphite could be changed into a round end when the iron matrix near the graphite end was rounded off by heat treatment. Thus, it is considered that the morphology of graphite precipitated in the solid phase is also dependent on the site where graphite precipitates. Here the site theory is proposed and the idea is based on the above.

CONCLUSIONS

1. The chunky graphite cell was much bigger than other types of graphite cells; the average size was approximately 0.8 mm^3 in 230 mm thickness of 36-ton casting. Chunky graphite was complicatedly interconnected and frequently branched in the cell. The trace of austenite dendrite arm was also observed in the cell.

2. Chunky graphite basically possessed the same substructure as CV and spheroidal graphite being composed with the graphite chips. Each graphite chip has a face of basal plane, a section of prism face, and the thickness of approximately 2.5 nm. This kind of substructure would be formed if carbon diffused on graphite through the austenite shell or thin melt channel.

3. Chunky graphite dominantly grows along the a-axis of the graphite hexagonal crystal, the same as other types of graphite in cast irons.

4. Mg segregated around all graphite nodules in austenite shell. This was not only graphite nodules in the spheroidal graphite structure, but also graphite nodules in the chunky graphite structure.

5. In case of chunky graphite structure, Mg, Ce, Al, P, S, Ti, O, and N segregated at the site between austenite dendrites and between austenite dendrite and shell. These sites were equivalent to the initial nucleation sites for chunky graphite. The Si-rich area was almost equal to the above austenites.

6. These segregated elements existed as inclusions except Mg. Mg was observed as the metallic state and inclusion. The metal Mg and inclusion were in contact with chunky graphite. Si was also segregated at inclusions.

7. The site theory was newly proposed to explain the graphite formation mechanism in liquid and solid state of cast iron. It was found that the chunky graphite formation mechanism could also be explained with the site theory, same as other graphite types.

8. According to the site theory, it is considered that the main cause for the chunky graphite formation is a lack of Mg gas bubble as the free surface in the melt and the condition is caused at thermal center of heavy section by the certain eutectic solidification pressure from the first solidified surface area.

9. Chunky graphite starts to form at austenite-residual melt, liquid Mg-residual melt, and inclusion-residual melt interface, or among all of them. However, these give only initial site for the chunky graphite nucleation. After the nucleation, austenite shell has the key to form chunky graphite.

ACKNOWLEDGMENTS

The authors would like to acknowledge Dr. H. Shingu and Dr. N. Inoyama of Kyoto University for their comments in assembling this manuscript. The authors would also like to acknowledge H. Takagi and K. Hada of GEOL Research Center in Tokyo for their cooperation in this study.

REFERENCES

1. H. Itofuji, Y. Kawano, S. Yamanoto, N. Inoyana, H. Yoshida, and B. Chang; "Comparison of Substructure of Compacted/Vermicular Graphite with Other Types of Graphite," *AFS Transactions*, vol 91, p 313 (1983).
2. H. Itofuji, Y. Kawano, N. Inoyama, S. Yamamoto, B. Chang, and T. Nishi; "The Formation Mechanism of Compacted/Vermicular Graphite in Cast Iron," *AFS Transactions*, vol 91, p 831 (1983).
3. N. Yingyi and Z. Zhu; "A Study of the Rare Earth Effect on Chunky Graphite Formation in Heavy-section Ductile Iron," *The Foundryman*, p 390 (Aug 1988).
4. J. Zhou, W. Schmitz, and S. Engler; "Untersuchung der Gefugebildung von Gußeisen mit Kugelgraphit bei Langsamer Erstarrung," *Giesserei-Forschung*, vol 39, Heft 2, p 55 (1978).
5. J. M. Motz and D. B. Wolters; "Uber Erstarrungsgefuge und Eigenschaffen in Dichwandigen Gußstucken aus Ferritischem Gußeisen mit Kugelgraphit-Teil 1: Mikroseigerungen," *Giesserei-Forschung*, vol 40, Nr. 2, p 69 (1988).
6. P. C. Liu, C. L. Li, D. H. Wu, and C. R. Loper, Jr.; "SEM Study of Chunky Graphite in Heavy-Section Ductile Iron," *AFS Transactions*, vol 91, p 119 (1983).
7. R. K. Buhr; "Vermiculite Graphite Formation in Heavy-Section Nodular Iron Castings," *AFS Transactions*, vol 76, p 497 (1968).
8. S. I. Karsay and E. Compomanes; "Control of Graphite Structure in Heavy Ductile Iron Castings," *AFS Transactions*, vol 78, p 85 (1970).
9. P. Strizik and F. Jeglitsch; "Contribution to the Mechanism of Formation of Chunky Graphite," *AFS International Cast Metals Journal*, vol 12, (Sep 23, 1976).
10. S. I. Karsay; *Production of Ductile Cast Iron 1*, p 41 (1976).
11. C. W. Thomas; "The Effect of Antimony on the Structure of Low-Magnesium Hypereutectic Irons Containing Proportions of Nodular Graphite," *BCIRA Journal*, vol 30, report No. 1453, p 36 (Jan 1982).
12. R. Schlvnsselberger, J. Daubmeier, and G. V. Grossmann; "Long Term Holding of Magnesium Treated Iron Melts," *Giesserei-Praxis*, Nr. 21, S320 (Nov 1983).
13. S. Yamamoto, B. Chang, Y. Kawano, R. Ozaki, and Y. Murakami; "Mechanism of Nodularization of Graphite on Cast Irons Treated with Magnesium," *Metal Science*, vol 12, p 239 (May 1978).
14. V. Oldfield; "Chill Reducing Mechanism of Silicon in Cast Iron," *BCIRA Journal*, vol 10, no 1, p 27 (Jan 1962).
15. L. Backerud, N. Nilsson, and M. Steen; *The Metallurgy of Cast Iron*, p 625 (1975).
16. T. Carlberg and H. Fredriksson; *Proceedings of Int. Conf on Solidification and Casting of Metals*, Sheffield, England (July 1977).
17. C. F. Walton and T. J. Oper; *Iron Castings Hand Book*, p 135 (1981).
18. D. M. Stefanescu and C. R. Loper, Jr.; "Effect of Lanthanum and Cerium on the Structure of Eutectic Cast Iron," *AFS Transactions*, vol 89, p 425 (1981).
19. J. F. Janowak and R. B. Gundlach; "A Modern Approach to Alloying Gray Iron," *AFS Transactions*, vol 90, p 847 (1982).
20. D. Pohl, E. Roos, and E. Scheil; *Giesserei-Technik*, vol 27, p 1513 (1960).
21. S. Yamamoto, B. Chang, Y. Kawano, R. Ozaki, and Y. Murakami, "Producing Spheroidal Graphite Cast Iron by Suspension of Gas Bubbles in Melts," *AFS Transactions*, vol 83, p 217 (1975).
22. Y. Lee and Y. Kawano; "Precipitation of Spheroidal Graphite During Cooling from Liquid State in Hyper Eutectoid Steel," *Journal of the Japan Institute of Metals*, vol 45, p 812 (1981).
23. Y. Lee and Y. Kawano; "Formation Mechanism of Precipitated Graphite Shapes in Hyper Eutectoid Steel," *Journal of the Japan Institute of Metals*, vol 45, p 948 (1981).
24. K. Hanawa, K. Achechi, Z. Hara, and T. Nakagawa; "Nodular Graphite Formation in P/M Products from Cast Iron Swarf Powder and Fe-Si-C Mixed Powders," *Trans. JIM*, vol 21, no 12, p 765 (1980).
25. Y. Kawano and T. Sawamoto; "Produce of Cast Iron with Fine Granular Graphite," *AFS Transactions*, vol 88, p 463 (1980).
26. S. I. Karsay; *Ductile Cast Iron 3*, p 73 (1981).